IJMTARC – VOLUME – V – ISSUE – 22, APR - JUNE, 2018 ISSN: 2320-1363

HIGH EFFICIENCY DC-DC CONVERTER WITH SOFT SWITCHING CAPABILITY FOR RENEWABLE ENERGY APPLICATIONS REQUIRING HIGH VOLTAGE GAIN

R.MONISHA[1], J. SIVAKUMAR[2]

[1] M.E.,SCHOLAR, DEPARTMENT OF EEE, RANIPETTAI ENGINEERING COLLEGE, T.K.THANGAL

[2] ASST PROFESSOR, DEPARTMENT OF EEE, RANIPETTAI ENGINEERING COLLEGE,T.K.THANGAL

ABSTRACT

In the last few decades, there has been a drastic increasing the demand for electricity this has led to rapid use anddepletion of fossil fuels. These factors have led theresearchers to renewable energy sources such as wind,solar PV and fuel cell stack. Solar Photovoltaic (PV) and fuel cell energy sources play a prominent role among the existing renewable sources poses major challenges such as Optimal utilization of the source due to their non-linear characteristics (e.g. Maximum Power Point Tracking in (MPPT) is required to track maximum available power from a PV source); They are usually operated at low output voltage levels (typ. 25-50V) because of safety issues. This makes their application to grid connected systems and even some stand-alone loads difficult because a large voltage boosting is required. It causes large peak current to flow on the input side, which adversely affects the magnetic components and results in high losses. Direct voltage step-up using high frequency transformer.

EXISTING METHOD

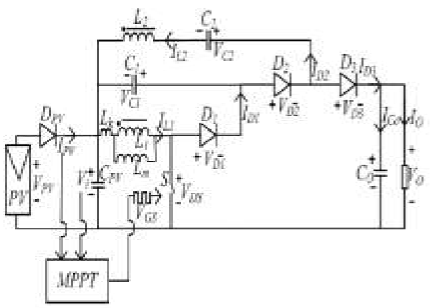

Fig: 1 TopologyEnergy conversion efficiency of solar PV is quite low (about 12-25%). Therefore, it is essential to use a highly efficient power conversion system to utilize the PV generated power to the maximum. The existing high gain consists of one passive clamp network, coupled inductor (L1, L2) and an intermediate capacitor apart from other components.The symbol Vpv represents the PV voltage applied to the circuit. S is the main switch

of the proposed converter. The coupled inductor's primary and secondary inductors are denoted by L1and L2. C1 and D1 represent the passive clamp network across L1. The capacitor Co is the output while D3 is the output diode. The voltage Vo is the average (DC) output across the load. The intermediate energy storage capacitor. C2 and the feedback diode D2 are connected on the secondary side.

Mode 1 (to-t1):

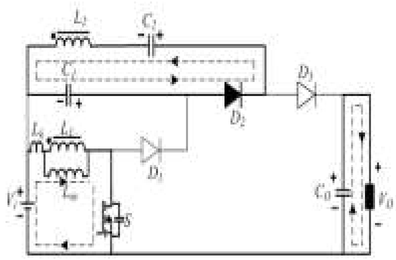

Fig:2Mode1

The switch (s) is turned on at the start of the converter operation. the current flows together the switch and the primary side of the coupled inductor (L1).Energizing the magnetizing inductance(Lm) of the coupled inductor current path is as shown in fig 1.the two diodes D1 and D3 are reverse biased. While D2 is forward biased during this mode. The intermediate capacitor,C2 is charged through D2 by L2 and capacitor,C1.

Mode 2 (t1, t2):

IJMTARC – VOLUME – V – ISSUE – 22, APR - JUNE, 2018

ISSN: 2320-1363

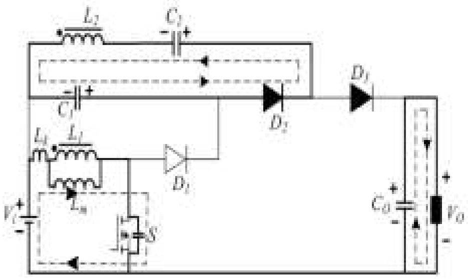

Fig :3 Mode2

The parasitic capacitance of the switch S is charged by the magnetizing current flowing through the inductor L1.The diode D2 remains forward biased and current continues to flow through this. Current path in this mode is shown fig2.

Mode3 (t2-t3):

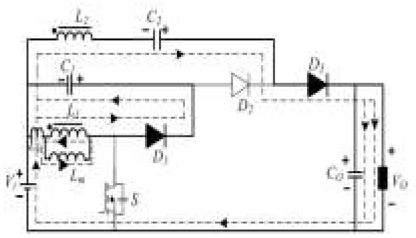

Fig: 4 Mode3

In this mode, diodes D1 and D3 become forward biased.D2 is reversed biased and its current become zero in this mode. The leakage energy stored in the primary side of the coupled inductor (L1) is recovered and stored in the clamp capacitor (C1) through diode D3.

Mode 4 (t3-t4):

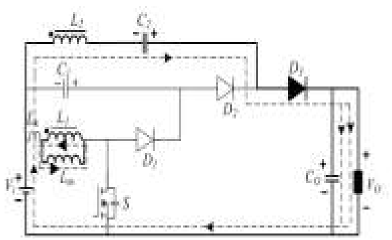

Fig: 5Mode4

This mode begins after the completion of recovery of the leakage energy from inductor (L1). The diode D1 now becomes reverse biased while diode D3 remains forward biased in this mode. The current flows from the input side to the output side to supply the load.

Mode 5(t4-t5):

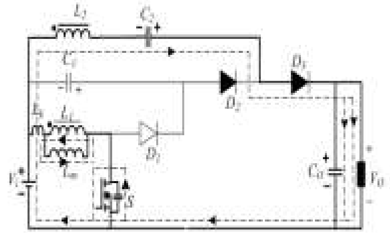

Fig: 6 Mode 5

This mode begins by turning on switch S. The leakage inductor energizes quickly using the full magnetizing current while the parasitic capacitance across the switch discharges in this mode. The two diodes D1 and D2 are in reversebiased conduction. The two diodes D1 and D2 are in reverse biased condition. The voltage (Vdc) across the switch 'S' cannot change instantaneously and decreases slowly. Thus there is little overlap of falling voltage and raising current and negligible switching loss at turn –on.

PROPOSED METHOD:

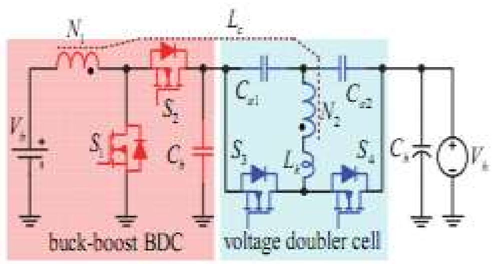

Fig: 7Proposed bidirectional DC-DC converter

The proposed high step-up/step-down BDC is shown in Fig, respectively. N1 and N2 are the primary and secondary windings of the coupled inductor Lace. From Fig. 1, it can be seen that the proposed BDC is a combination of the conventional buck-boost BDC and a voltage doubler cell. The magnetizing inductance Lm of the primary winding of the coupled inductor Lc is used as a filter inductor of the buck-boost BDC, while the secondary winding of the coupled inductor is inserted into the voltage doubler cell to improve the voltage conversion ratio of the BDC. Since the two switch bridges composed of S1&S2 and S3&S4 are connected in series, the high voltage Vh is divided into two parts and shared by the two switch bridges, the voltage stresses on the active switches S1-S4 are reduced.

The proposed BDC topology can be divided into two parts. The equivalent circuits of the two parts are illustrated in Fig. 2, where it is shown that the equivalent circuit between the battery Vb and the capacitor Cb is a conventional buck-boost BDC, while the equivalent circuit between the capacitor Cb and the high side source Vh is a DAHB BDC. Therefore, the proposed BDC is derived by integrating the buck-boost BDC and the DAHB BDC through sharing the low-side switches, S1 and S2, and the capacitor Cb. It has been known that the best operation condition for the DAB BDC is that the voltages on the two sides of the DAB BDC are well matched [20]-[22]. In this case, the highest efficiency can be realized because the circulating current is minimized and soft-switching of switches is always achieved. Fortunately, voltage matching control can be achieved with the unique structure of the proposed BDC. Because the output voltage, VCb, of the buck-boost BDC is used as the input voltage of the DAHB BDC, the voltages on the two windings, N1 and N2, of the DAHB BDC can be controlled and matched with the turn ratio of the coupled inductor. To achieve the voltage matching, the voltage VCb is controlled by the buck-boost BDC to satisfy the following equation:

$$\frac{V_{Cb}}{V_h - V_{Cb}} = \frac{N_1}{N_2} = \frac{1}{n}$$

Close observation indicates that the proposed BDC has the following features.

(1) Because the voltages on the two sides of the DAHB BDC are exactly matched to the turn’s ratio of the coupled inductor, the circulating current is minimized and the soft-switching of all the switches can be always achieved.

(2) High step-up/step-down voltage conversion ratio is achieved easily with the coupled inductor and the output-series configuration.

(3) Wide voltage range regulation can be realized with the PWM controlled buck-boost BDC. Since the efficiency of the PWM controlled buck-boost BDC is not sensitive to the voltage range, high conversion efficiency within wide battery voltage range is expected.

(4) The circuit configuration of the proposed BDC is simplified by sharing the two switches, S1 and S2, between the buck-boost BDC and the DAHB BDC. More importantly, with the help of the DAHB BDC, the two switches S1 and S2 that belong to the buck-boost BDC can realize ZVS as well.

(5) The inductor Lk can be partly or fully implemented with the leakage inductance of the coupled inductor, which results in effective utilization of parasitic parameters and high power density.

OPERATION OF THE PROPOSED CONVERTER

The proposed high step-up/step-down BDC shown in Fig. is analyzed to verify the feasibility of the proposed topology and control method. The switches S1 and S2 are driven complementary, while S3 works complementarily with S4. S1and S3 share the same duty cycle D, and D is used to regulate the voltage on the capacitor Cb, VCb. So the voltages VCb and Vh are always matched and satisfy (1). The phase-shift angle, φ, between S1 and S3 is utilized to regulate the value and direction of the transferred power of the BDC. According to the direction of the power flow, the BDC has two operation modes, i.e. step-up mode and step-down mode. The converter operates in the step-up mode if the energy is transferred from the low voltage side, Vb, to the high voltage side, Vh, whereas, the converter operates in the step-down mode if the power flow is reversed. In the step-up mode, the driving signal of S1 always leads the driving signal of S3, which means the phase-shift angle φ>0. On the other hand, the driving signal of S1 always lags the driving signal of S3 and the phase-shift angle φ<0 when the converter operates in the step-down mode..

IJMTARC – VOLUME – V – ISSUE – 22, APR - JUNE, 2018

ISSN: 2320-1363

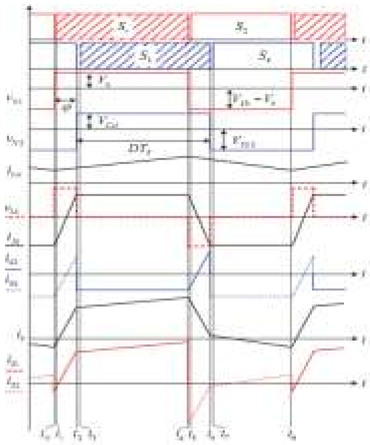

Fig: 8 key waveforms of the proposed BDC, the step-up mode

Mode 1[t0, t1]:

Before t0, the switches S2 and S4 are ON, and both the current ib and iLk are negative. At t0, S2 is turned OFF. The body diode of S1 is ON due to the negative current of ib.

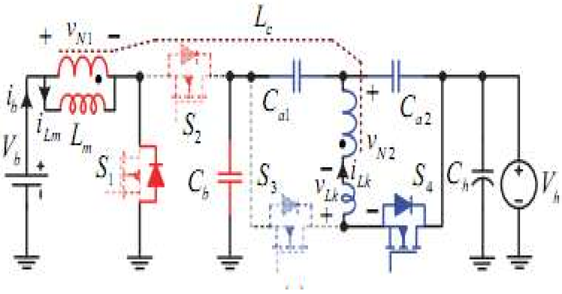

Fig.9 Mode1

Mode 2[t1, t2]:

At t1, S1 is turned ON with zero voltage switching (ZVS). During the Stage 1[t0, t1] and the Stage 2[t1, t2], the currents iLm and iLk increase linearly due to the positive voltage on the inductors L and L.

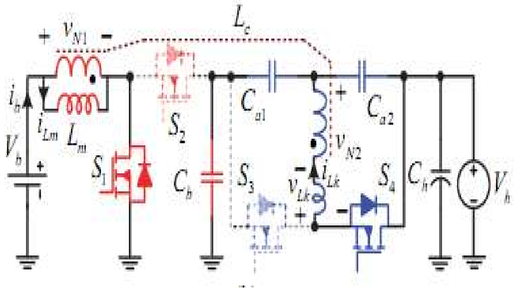

Fig: 10 Mode2

Mode 3[t2, t3]:

At t2, S4 is turned OFF, the body diode of S3 is ON due to the positive value of iLk.

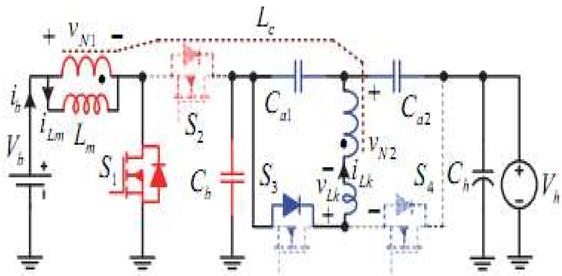

Fig: 11 Mode3

Mode4[t3, t4]

At t3, S3 is turned ON with ZVS because S3 is operated as a synchronous switch in this Stage. During the Stage 3[t2, t3] and the Stage 4[t3, t4], the battery is discharged and supplies power to the load. So the inductor Lm is charged by Vb, and iLm keeps increasing linearly. And iLk is expressed as follows.

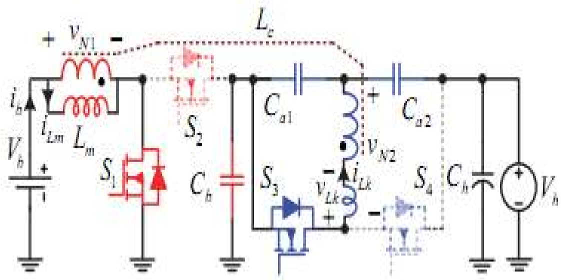

Fig: 12 Mode 4

Mode 5[t4, t5]:

IJMTARC – VOLUME – V – ISSUE – 22, APR - JUNE, 2018

ISSN: 2320-1363

At t4, S1 is turned OFF, and the body diode of S2 is ON due to the positive values of iLm and iLk.

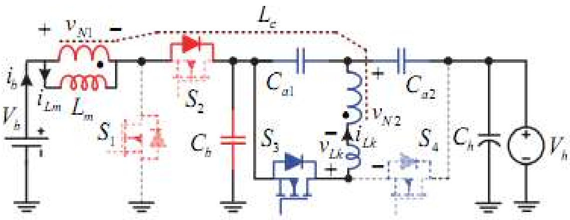

Fig: 13 Mode 5

Mode 6[t5, t6]:

At t5, S2 is turned ON with ZVS. ZVS of S5 can be always achieved because the current in S5 is negative and S operates as a synchronous switch in this Stage.

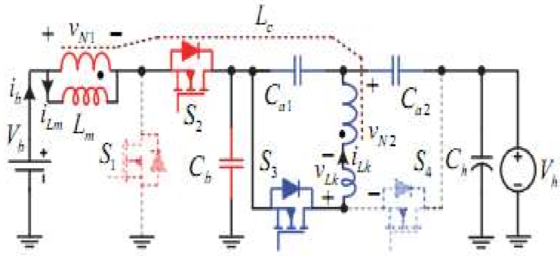

Fig: 14 Mode6

Mode 7[t6, t7]:

At t6, S3 is turned OFF and the body diode of S4 conducts because of the negative value of iLk.

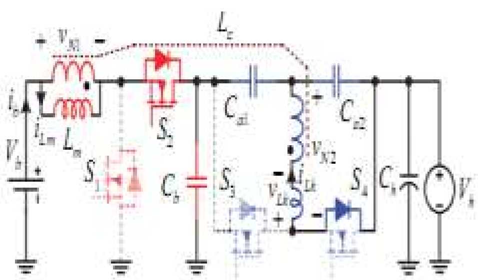

Fig: 15 Mode 7

Mode8[t7, t8]:

At t7, S4 is turned ON with ZVS.

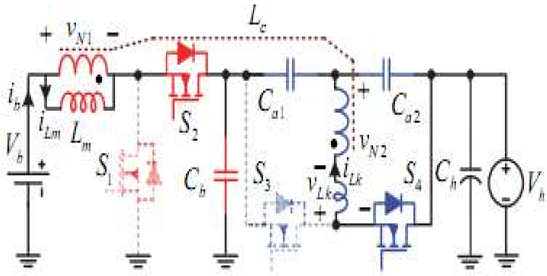

Fig: 16 Mode 8

SIMULATION RESULTS

Simulation has become a very powerful tool on the industry application as well as in academics, nowadays. The objective of this chapter is to describe simulation of impedance source inverter with R, R-L and RLE loads using MATLAB tool.

Simulation results

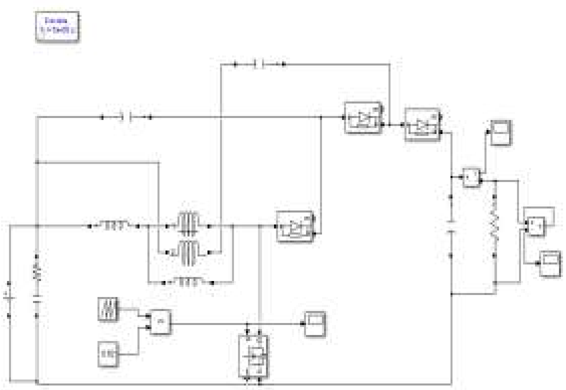

Fig:17 Matlab Implementation

Its consists of DC input voltage and four diode are connected to drive circuit and Inductances are placed between them . it has four capacitance are connected near connected to coupled inductance and storage capacitance .is input voltage in 12 V and output voltage in90 V. drive unit is used amplify voltage signal.

Input voltage(V)

IJMTARC – VOLUME – V – ISSUE – 22, APR - JUNE, 2018 ISSN: 2320-1363

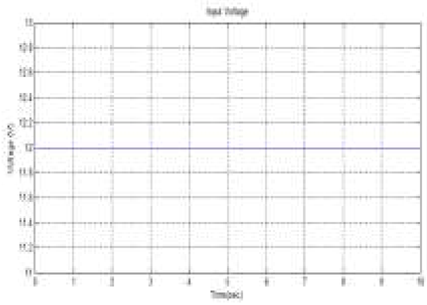

Fig:18Input voltage of converter

4.2.3LOAD VOLTAGE(V)

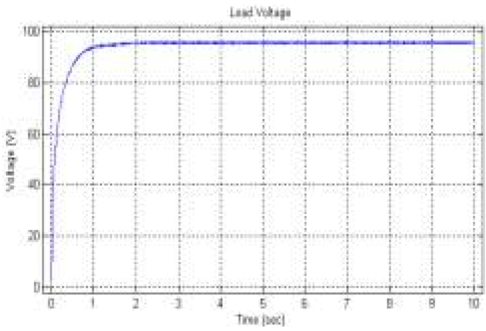

Fig:19Load Voltage of Existing converter

LOAD CURRENT(A)

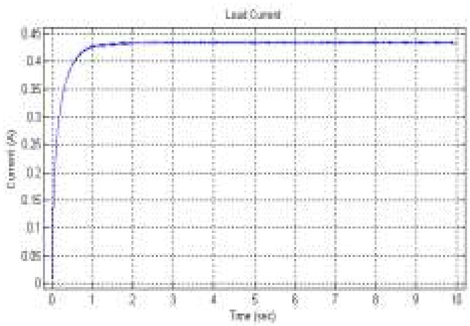

Fig:20Load Current of Existing converter

Proposed Implementation

Open loop response

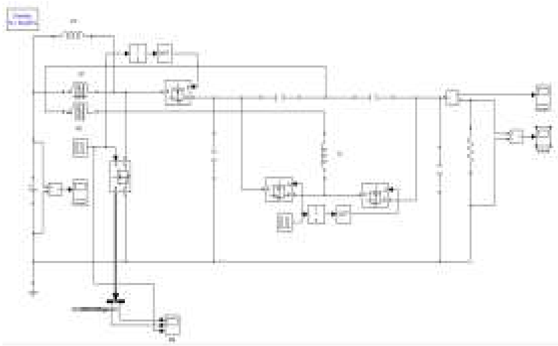

Fig. 21 Matlab Implementation Circuit of Proposed High Step up Converter System in open loop

Its consists of DC source voltage and four MOSFET are connected to dive circuit and inductances are placed between them it has four capacitance are connected to the open loop response connected pulse generator the input voltage 12V and output voltage 120V and output current 1.2 A.

LOAD VOLTAGE (V)

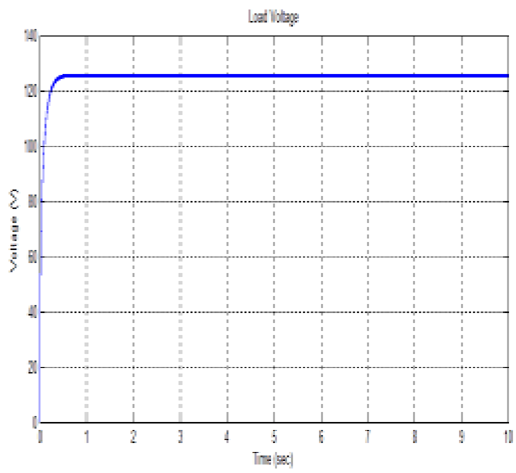

Fig. 22 Load Voltage of High step up converter in open loop

LOAD CURRENT(A)

ISSN: 2320-1363

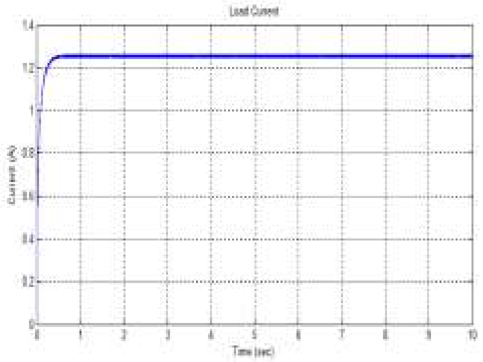

Fig. 23 Load Current of High step up converter in open loop

The output current is drawn between the current(A)and time(sec).it reaches the maximum current 1.2A.

SOFT SWITCH

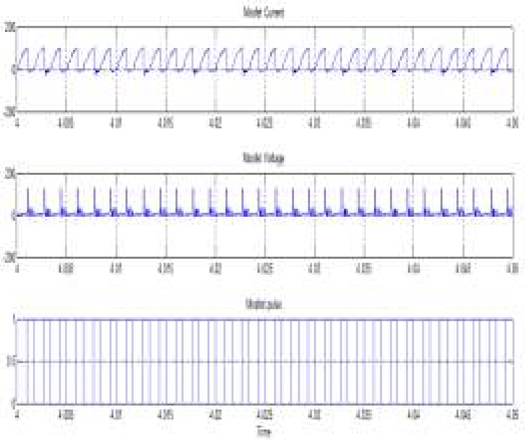

Fig. 24 Soft Switching Performance

Closed loop response

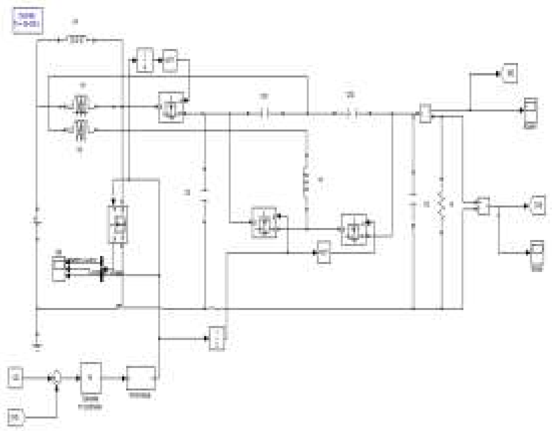

Fig. 25 Proposed High Step up Converter System in closed loop

Its consists of DC source voltage and four MOSFET are connected to dive circuit and inductances are placed between them it has four capacitance are connected to the closed loop response connected PIcontrollerfor buck boost converter.

INPUT VOLTAGE(V)

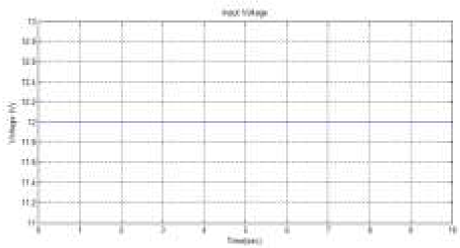

Fig. 26 Input voltage of High step up converter in closed loop

In input voltage using. The input graphs are shown above. The graph is drawn between input voltage Vs time. The input voltage 12V

OUTPUT VOLTAGE(V)

IJMTARC – VOLUME – V – ISSUE – 22, APR - JUNE, 2018 ISSN: 2320-1363

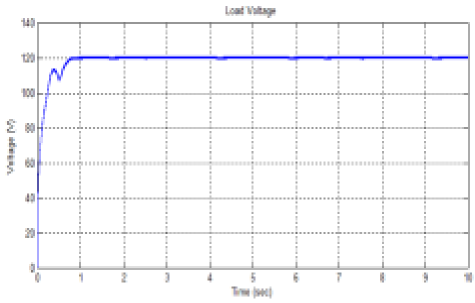

Fig.27 Load Voltage of High step up converter in closed loop

OUTPUT CURRENT(A)

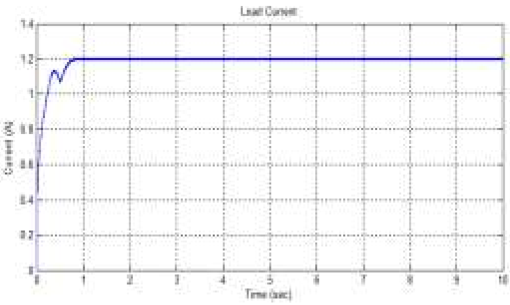

Fig. 28 Load Current of High step up converter in closed loop

4.3.9 SOFT SWITCH

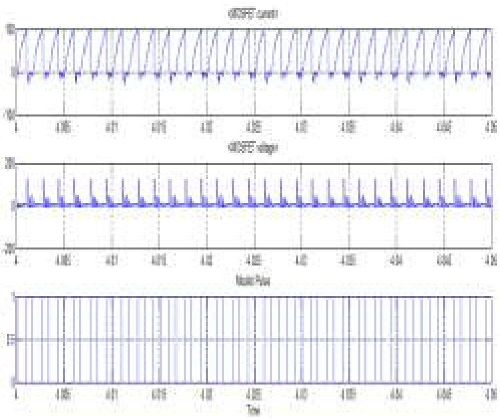

Fig. 29 Soft Switching Performance of High step up converter in closed loop

CONCLUSION

In this project, novel high efficiency high step-up/step-down bidirectional DC-DC converter is proposed by integrating a dual-active half-bridge (DAHB) BDC into the conventional buck-boost BDC. The voltage stresses of switches have been reduced and the voltage conversion ratio has been increased by connecting the outputs of the buck-boost BDC and the DAHB BDC in series. Voltage matching control for the DAHB BDC is achieved by regulating the switches duty cycles of the buck-boost BDC. As a result, the voltages on the two sides of the DAHB BDC are always matched to reduce the conduction losses and improve the soft-switching performance of the DAHB BDC. Power flow regulation is achieved by adopting phase shift control to the DAHB BDC. Furthermore, ZVS soft switching is realized for all of the switches to lower the switching losses. Finally, the effectiveness of the proposed BDC topology and control is verified using simulation in MATLAB/Simulink platform. Simulation results indicate that the proposed solution is a good candidate for high efficiency energy storage system applications with steep voltage gain and wide battery voltage range.

REFERENCES

[1] J.G. de Matos, F. S. F. e Silva, L. A. de S Ribeiro, "Power control in AC isolated microgrids with renewable energy sources and energy storagesystems," IEEE Trans. Ind. Electron., vol. 62, no. 6, pp. 3490-3498, June 2015.

[2] X. Lu, K. Sun, J. M. Guerrero, J. C. Vasquez, L. Huang, "Double-Quadrant State-of-Charge-Based Droop Control Method for Distributed Energy Storage Systems in Autonomous DC Microgrids," IEEE Trans. Smart Grid , vol. 6, no. 1, pp. 147-157, Jan. 2015.

[3] M. Vasiladioties, A. Rufer, "A modular multiport power electronic transformer with integrated split battery energy storage for versatile ultrafast EV charging stations," IEEE Trans. Ind. Electron., vol. 62, no. 5, pp. 3213-3222, May 2015.

[4] D. Debnath, K. Chatterjee, "Two-stage solar photovoltaic-based stand-alone scheme having battery as energy storage element for rural deployment," IEEE Trans. Ind. Electron., vol. 62, no. 7, pp. 4148-4157, July 2015.

[5] T.-J. Liang, J.-H. Lee, "Novel high-conversion-ratio high-efficiency isolated bidirectional DC-DC

IJMTARC – VOLUME – V – ISSUE – 22, APR - JUNE, 2018

ISSN: 2320-1363

converter," IEEE Trans. Ind. Electron., vol. 62, no. 7, pp. 4492-4503, July 2015.

[6] D.-Y. Jung, S.-H.Hwang, Y.-H.Ji, J.-H.Lee, Y.-C.Jung, and C.-Y. Won, "Soft-switching bidirectional DC/DC converter with a LC series resonant circuit," IEEE Trans. Power Electron., vol. 28, no. 4, pp. 1680-1690, Apr. 2013.